FINAL REPORT

Student Name: Ahmed Gaballah

Cycle:XXX (externally funded from the EXTATIC Erasmus mundus program)
Address: 1- Department of Information engineering University of Padova, Italy
2- University Colleague of Dublin (UCD), Ireland.

Supervisor: Prof. Piergiorgio Nicolosi (Padova University) Department of Information Engineering.
Dr. Tom McCormack and Fergal Oreilly University Colleague of Dublin (UCD), Ireland

Thesis title (final): EUV Multilayer optical coatings development

PART 1 - COURSES, CONFERENCES AND MOBILITY

Courses for Ph.D. students

- Statistical Methods /**Prof. Finesso** (DEI – University of Padova)
- X-ray techniquesfor material analysis / **Prof.Bazzan** (Physics Dep. University of Padova)
- EUV Optics / **Prof. Nicolosi** (EXTATIC Modules) (DEI – University of Padova)
- Meteorology of EUV and Soft X-rays /**Prof. Juschin** (EXTATIC Modules) (RWTH, Aachen University, German)
- Italian language course (EXTATIC Modules) (Language and translation center – University of Padova)

Summer schools, short courses, tutorials

- Italian language course Università per Stranieri di Siena,Italy.
- Accepted Proposal no. 20155288 and awarded 18 operational shifts on the BEAR beamline, together with the related technical and organizational support.
- accepted proposal no. 20160207 and awarded 15 operational shifts on the BEAR beamline, together with the related technical and organizational support.

Seminars

- PTB Seminar VUV and EUV Metrology "EUV ellipsometric measurements: a proof of concept" 19-20 Octobor 2017 at PTP Berlin, Germany **(Oral Presentation).**

Participation to International Conferences and Workshops

Extatic Workshops **"**EUV Multilayer optical coatings development**"** at MUT (Warsaw Poland), 20 - 24 October 2014 **(Oral Presentation).**

Extatic Workshops “Optical characterization of reflective quarter wave retarder in FUV-EUV range” 11 - 15 January 2016 in the University of Southampton, UK. **(Oral Presentation**).

SPIE conference astronomical telescope and instrumentation in Edinburge, United Kingdom Jun 26-30, 2016 **(Poster Presentation).**

COST Action orkshops: MP1203 (X-ray optic metrology) , Sept. 19-21, 2016 Athens, Greece. **(Poster Presentation)**.

Workshop of Multilayer and neutron scattering 10-11 November 2016 University of Twente, Netherland **(Poster Presentation)**.

Extatic Workshops “Optical and structural characterization of reflective quarter wave plates for EUV range” 16-20 January 2017 at the International Centre for Theoretical Physics in Trieste, Italy. **(Oral Presentation).**

SPIE conference: Synergy between Laboratory and Space, Prague 24-27 April **2017 (Poster Presentation).**

SPIE conference: Damage to VUV, EUV, and X-ray Optics, Prague 24-27 April **2017 (Poster Presentation).**

PTB Seminar VUV and EUV Metrology "EUV ellipsometric measurements: a proof of concept" 19-20 Octobor 2017 at PTP Berlin, Germany **(Oral Presentation).**

Other learning activities

- Academic writing skills course (UCD).
- Management of 3D printing (self-learning).
- Manipulating and designing 3D models by Autodesk inventor and Blender software (self-learning).
- References editing and citation management by Endnote and Mendeley software (self-learning).

Mobility periods

My mobility path was arranged for the starting on 25th June 2017 at University Colleague of Dublin (UCD), Ireland for minimum 6 moths. The activates planed during this period are data analysis for the measurements made at the home university (Padova, Italy), writing the PhD dissertation, I was enrolled in an experiment based on soft x-ray produced by Laser Produced Plasma

PART 2 - RESEARCH ACTIVITY

The scientific activities in the last two years focused on design, deposition and characterization of single/multilayers (MLs) designed for FUV-EUV polarimetry applications as Quarter Wave Retarder and optical polarizer.

Aim of work

Designing and studying an EUV polarimetric apparatus based on multilayer structures as QWR works within a suitably wide spectral range (88-160 nm) where some important spectral emission lines are as the hydrogen Lyman alpha 121.6 and Oxygen VI (103.2 nm) lines. The design covered with a protective capping layer to avoid oxidation and contamination to improve stability and reflectivity. Such design could be particularly useful as analytical tools in EUV-ellipsometry field. In addition, the phase retarder element could be used in other experimental applications for generating EUV radiation beams of suitable polarization or for their characterization.

1. Introduction

Great interest and efforts have been recently paid to produce linearly and circularly polarized light in vacuum ultraviolet (VUV) and extreme ultraviolet (EUV) spectral ranges [1]. In space, polarimetry plays an important role for understanding the physical processes of the coronal plasma in the energy transfer from the inner parts of the sun to the outer space [2]; in photolithography, the contrast between the lowest and highest intensity is considerably enhanced by using linearly polarized light source when compared with unpolarized ones [3]; then circular dichroism spectroscopy [4], magneto-optical spectroscopy [5], and spectroscopic ellipsometry [6] are only some of other examples requiring polarimetry.

In the materials science, ellipsometry is considered one of the promising and superior technique for revealing the optical and structural properties of materials, since linearly and circularly polarized radiations are very sensitive to the interaction of light with electrons of materials and compounds [7,8]. Due to its favorable advantages, including that the method is not invasive and can give information about the sample with high-precision, spectroscopic ellipsometry has been studied in a wide spectral range from the infrared (IR) to the ultraviolet (UV). Optical systems based on the combination of optical polarizers, quarter-wave retarders, and optical analyzers [9] are available for this purpose.

The experimental and theoretical methods based on the Stokes formalism and the Mueller matrix calculus can be also extended to VUV and EUV light [10]. Several approaches have been used and several devices implemented at large scale facilities, such as synchrotron and free electron laser [11–15], for measuring the polarization state of VUV and EUV light. The first reported study above 6 eV was achieved at large scale facilities by using linearly polarized synchrotron radiation with dedicated insertion devices as triple-reflection polarizers [16]. However, the access to large scale facilities needs financial support and experiment proposals approval for beam time scheduling. Therefore, laboratory-based experimental systems are highly desired as good option to expensive and time consuming facility for fast, cheap and reliable preliminary experiments.

To produce circular or elliptical EUV polarization at small scale laboratory, a phase retarder element is needed [17–21]. However, as we move toward shorter wavelengths as problems arise since it is difficult to find suitable materials for fabrication of polarizer, QWRs, and phase retarders. In fact, all materials become highly absorbing in that spectral range and some problems arise for the control of the layers thickness and the contamination effects.

For example, reflective mirrors based on aluminum single layer introduce a suitable phase difference between the two-reflected TE and TM perpendicular polarized components over a relatively large EUV spectral range [22]. Furthermore, the presence of aluminum oxide Al_2O_3 due to the reaction with air strongly influences the optical properties of the film. In fact, the oxide layer has very high absorption in VUV range reducing the reflectance of the aluminum in this region and also affecting the phase difference [23].

In this paper, we will discuss the improvements and the implementation of the EUV reflectometer facility located in the Institute for Photonics and Nanotechnologies-CNR Padua (Italy). The system coupled with an EUV linear polarizer for performing EUV ellipsometry in 90-160 nm spectral range, has been used for the characterization of a single layer of aluminum as quarter wave retarder. The whole system consisting of the reflectometer and the polarizer can be a very promising laboratory system to characterize phase retarders, polarizers, and other optics in the VUV and EUV region and to investigate the properties of thin films and optical coatings. In addition, the phase retarder mirror based on aluminum and used in this

experiment, could be proposed for characterizing and controlling the polarization state of EUV radiation beams.

2. Experimental realization

2.1 VUV-EUV normal incidence reflectometer

A schematic diagram of the normal incidence reflectometer at CNR Padua [24] is shown in Fig.1. A 600 grooves/mm toroidal Pt-coated grating with a main radius of 0.5 m and 25° subtended angle between the entrance and the exit slits drives the light to a toroidal mirror. The toroidal mirror working at 45° incidence angle reflects the monochromatic radiation on the sample placed in the experimental chamber together with the polarizer and the detector. The samples, and the detector are mounted on movable holders in a θ-2θ configuration to allow measurements at different angles of incidence. In this experiment, the EUV radiation

was produced by a deuterium lamp with MgF_2 window emitting the strong 121.6 nm line superimposed on a spectrally continuous weaker emission [25]. Other lamps can be coupled to the system for covering the 90-160 nm spectral region. The beam impinging the sample is partially linearly polarized due to the multiple reflections. The light is allowed to pass through the four-reflection polarizer (FRP) rotating counter-clockwise with respect to the beam propagation direction, and the modulated intensity is gathered by the channel electron multiplier (CEM KBL10/90) manufactured by Sjuts Optotechnik [26].

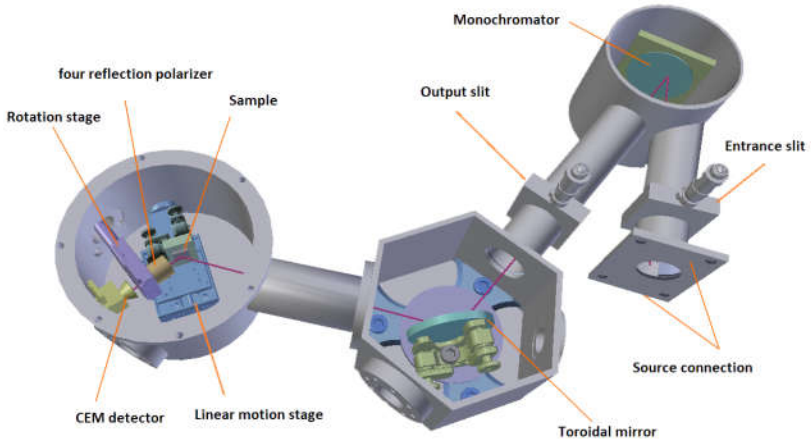

Fig.1. The VUV-EUV normal incidence reflectometer Facility located at CNR–IFN, Padua, Italy.

The samples are mounted on a linear movable stage to be extracted from or inserted in the radiation beam path and to allow the measurement of the incident and reflected intensity. As we have just pointed out, the incoming beam has a considerable polarization degree due to the geometrical arrangements of the diffraction grating and toroidal mirror. Then, in order to fully characterize the system, the measurements were performed at different orientations of the experimental chamber. The details of the test campaigns are discussed in the following sections.

2.2 Opto-Mechanical design of the polarizer (FRP)

In order to characterize the polarization state of the beam delivered by the EUV reflectometer, we manufactured a polarizer optimized for H-Lyman alpha line at 121.6 nm. It is a four-reflection linear polarizer designed and fabricated by using gold coated mirrors consisting of 200 nm thick films deposited by thermal evaporation on Si substrate; for a good adhesion of the gold, a 3-nm layer of chromium was e-beam evaporated between the substrate and the film. The design guarantees that the performances of the polarizer are relatively good even on an extended spectral range from 40 nm to 160 nm. A schematic of the polarizer design is shown in Fig. 2a. A special holder for mounting two couples of parallel mirrors has been manufactured in order to preserve the propagation direction of the incident beam after reflection. The mirrors, having dimension of 10 mm × 32 mm, are mounted with 60◦ normal incidence angle. The optical polarizer mounting system consists of two parts where the four mirrors are glued on four plane reference surfaces secured together by using screws (Fig. 2b). The device is mounted on vacuum compatible rotational

stage (Rs-40 Physik Instrument, with the minimum angular step size of 0.0025^0) [27], the total assembly of the polarizer combined with the rotation stage is shown in Fig. 2c. The transmitted beam intensity was collected by the channel electron multiplier (CEM) as it was already specified.

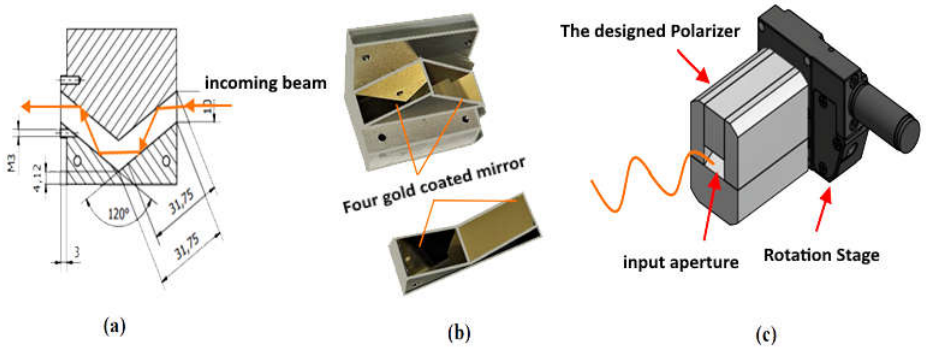

Fig. 2. (a) Design of four reflecting mirrors polarizer consisting of two halves, (b) all mirrors consisting of 200 nm layer of Au on Si substrate are glued onto the machined surfaces. (c) Overall shape of four reflection polarizer attached to the rotation stage.

We selected gold as reflective coating because it is a good reflector in this range, it is very stable and the optical constants are well known. However, a single gold surface at the Brewster angle of incidence is not enough for reaching high extinction coefficient.

The calculated reflectance R_s and R_p of the two orthogonal TE and TM polarization components versus wavelengths for different materials suitable as reflective coating for the linear polarizer are reported in Fig. 3a, together with the extinction ratio $\frac{R_s}{R_p}$ (Fig.3b). As it is confirmed by the curves in Fig. 3b, the gold coated polarizer works properly for different wavelengths from VUV to EUV range with a relatively good extinction ratio in the wide range of 65 nm-170 nm. However, it can be extended to wavelength shorter than 60 nm, although showing reduced performances.

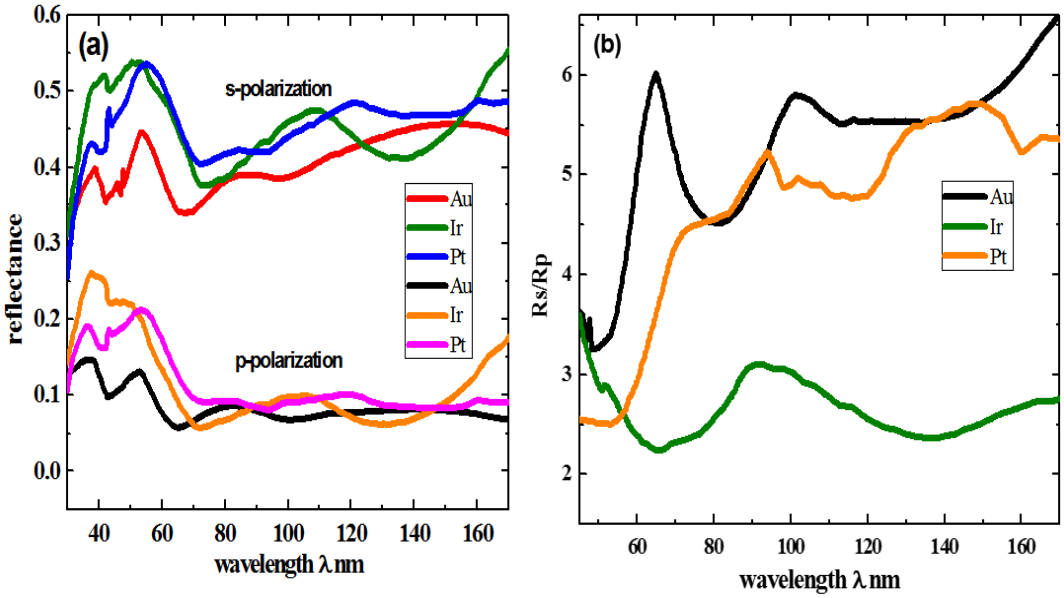

Fig. 3. (a) Calculated reflectance R_s and R_p versus wavelengths at normal incidence angle of 60^0; (b) ratio $\frac{R_s}{R_p}$ of Au, Ir, and Pt coatings on Si substrate for different wavelengths.

3. Experimental results

3.1 Stokes Parameters and Mueller Matrix Formalism

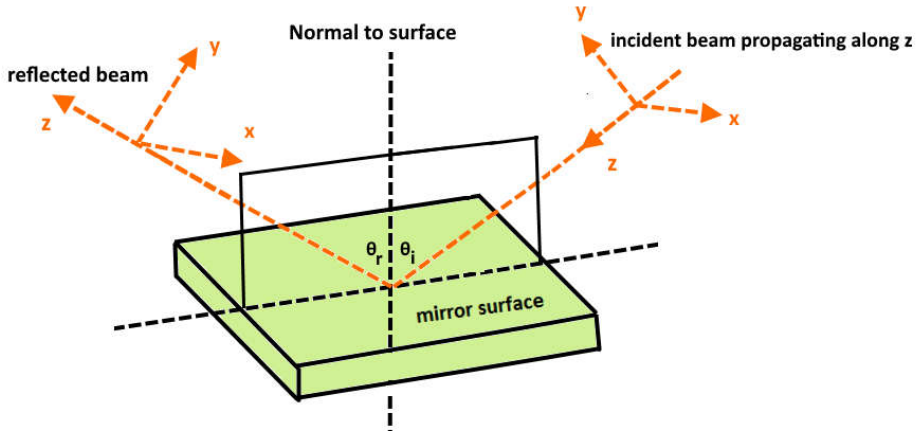

Fig. 4. The reference system used in the experiment. Incident linearly polarized light with electric field vector $\boldsymbol{E}_i$ propagates along the z axis, suitably chosen values of the incident angle θ_i and rotation angle θ.

Before explaining the method applied for the characterization of the light beam coming from the reflectometer and impinging the sample, we recall some basic concepts related to the use of the Stokes formalism and Mueller calculus. The polarization state of a light beam can be described by the Stokes formalism [10]. In the reference system defined in Fig.4 the electric vector E of monochromatic electromagnetic wave travels along the z-axis. In the general case, we can decompose the vector into $\boldsymbol{E}_x$ and $\boldsymbol{E}_y$ components, respectively along the x and y directions [28]. The Stokes parameters characterize the light beam in terms of intensities and phase difference δ:

$$\begin{pmatrix} S_0 \\ S_1 \\ S_2 \\ S_3 \end{pmatrix} = \begin{pmatrix} E_{0x}^2 + E_{0y}^2 \\ E_{0x}^2 - E_{0y}^2 \\ 2E_{0x}E_{0y}\cos\delta \\ 2E_{0x}E_{0y}\sin\delta \end{pmatrix} \qquad (1)$$

where the first parameter S_0 is the total irradiance of the light beam, the parameter S_1 describes the amount of horizontal or vertical linear polarization, the parameter S_2 describes the amount of +45° or −45° linear polarization, while the parameter S_3 describes the amount of right or left circular polarization, and $\delta = \delta_x - \delta_x$ is the phase difference between the two components. The Stokes parameters enable us to describe the degree of polarization P for any state of polarization by the definition:

$$P = \frac{S_{pol}}{S_{tot}} = \frac{\sqrt{S_1^{\,2} + S_2^{\,2} + S_3^{\,2}}}{S_0} \qquad (2)$$

When the beam goes through an optical element its polarization changes [10], then the Stokes parameters change. The effect of the optical element is described by the related Mueller matrix of the optical system and the Stokes vector of the output light is given by:

$$S^{\sim} = M.S \qquad (3)$$

where M *is 4x4* Mueller matrix associated to the optical system. The concept of the Mueller calculus can be extended to complex optical equipment, composed by a set of elements; the equivalent Mueller matrix of the whole system is given by the product of the Mueller matrix of each element.
In case of the four-reflection linear polarizer used in the experiment, the Müller matrix is:

$$M_{FRP}=\begin{pmatrix} \frac{|r_s|^8+|r_p|^8}{2} & \frac{|r_s|^8-|r_p|^8}{2} & 0 & 0 \\ \frac{|r_s|^8-|r_p|^8}{2} & \frac{|r_s|^8+|r_p|^8}{2} & 0 & 0 \\ 0 & 0 & r_s^4 r_p^4 & 0 \\ 0 & 0 & 0 & r_s^4 r_p^4 \end{pmatrix} \quad (4)$$

The terms r_s^8 and r_p^8 come out because the polarizer is based on four-reflection mirrors. The polarizer can rotate by an angle (θ) around its axis counter-clockwise with respect to the beam propagation direction and the modulated intensity is collected by the channel electron multiplier (CEM KBL 10RSR). A schematic diagram of the arrangement is shown in Fig.1. In the figure, also the sample on the removable stage is shown.

According to the Mueller calculus, the Mueller matrix of the rotated four reflection polarizer is [29]:

$$\begin{pmatrix} \frac{|r_s|^8+|r_p|^8}{2} & \frac{|r_s|^8-|r_p|^8}{2}\cos 2\theta & \frac{|r_s|^8-|r_p|^8}{2}\sin 2\theta & 0 \\ \frac{|r_s|^8-|r_p|^8}{2}\cos 2\theta & \frac{|r_s|^8+|r_p|^8}{2}\cos^2 2\theta + r_s^4 r_p^4 \sin^2 2\theta & \frac{|r_s|^8+|r_p|^8}{2}\cos 2\theta.\sin 2\theta - r_s^4 r_p^4 \sin^2 2\theta.\cos 2\theta & 0 \\ \frac{|r_s|^8-|r_p|^8}{2}\sin 2\theta & \frac{|r_s|^8+|r_p|^8}{2}\sin 2\theta.\cos 2\theta - r_s^4 r_p^4 \cos 2\theta.\sin 2\theta & \frac{|r_s|^8+|r_p|^8}{2}\sin^2 2\theta + r_s^4 r_p^4 \cos^2 2\theta & 0 \\ 0 & 0 & 0 & r_s^4 r_p^4 \end{pmatrix} \quad (5)$$

where θ is the rotation angle of the polarizer around the beam propagation axis.

The output intensity of the light beam propagating through the polarizer and collected by the detector is:

$$\tilde{S}_0 = \frac{1}{2}\left[\left(|r_s|^8+|r_p|^8\right)S_0 + \left(|r_s|^8-|r_p|^8\right)S_1\cos 2\theta + \left(|r_s|^8-|r_p|^8\right)S_2\sin 2\theta\right] \quad (6)$$

The Stokes parameters S_0, S_1, and S_2 can be retrieved by investigating the output signals coming from the rotating polarizer without the sample on the optical path (Fig. 1). S_0 is the total intensity that we can assume normalized.

In order to determine the Stokes parameters S_1 and S_2 we performed the measurements by rotating the experimental chamber by 135° clockwise around the direction defined by the beam propagation. Then, the light entering was -45° linearly polarized. We used a MATLAB code developed accordingly to the Eq. 6, in order to determine S_1 and S_2 by fitting procedure. The reflectance values of the gold mirrors were experimentally measured to reduce the number of fitted parameters.

Fig. 5 shows the measured and fitted data against the rotation angle of the polarizer at 121.6 nm wavelength in two polarization states:

a) almost fully polarized light along the y axis (Fig. 5a);
b) almost fully -45° polarized light as described by the polarization ellipse (Fig. 5b).

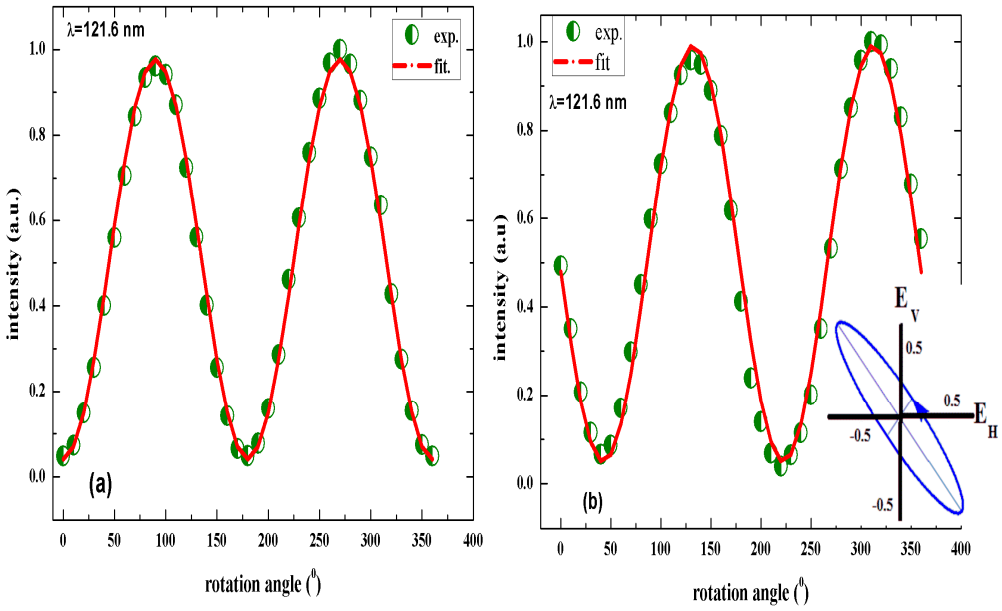

Fig. 5. a) Measured values and the fitted curve of the modulated intensity versus the rotation angle of the polarizer at 121.6 nm in case of almost fully polarized light along the y axis; b) measured values and the fitted curve of the modulated intensity versus the rotation angle of the polarizer at 121.6 nm in case of almost fully -45° polarized light as described by the polarization ellipse. Inset shows the polarization state of the light impinging the sample.

Table 1. The Stokes parameter of the incident beam at wavelengths 121.6 nm

Stokes Vector	a) almost fully polarized light along the y axis	b) almost fully -45° polarized light
S_0	1	1
S_1	-0.92	-0.006
S_2	-0.002	-0.90

It is worth mentioning the reversal role of S_1, and S_2 by changing from polarization state a) to b). S_1 (S_2 in b)) is <<1, while S_2 (S_1 in b)) is -0.92 determined with ~2% uncertainty.

3.2 Structure properties of Aluminum phase retarder

In order to estimate the potential of the table top ellipsometer system, a phase retarder element was introduced along the optical path (see Fig. 1) [9]. An aluminum mirror was used as a phase retarder. It consists of 100 nm thickness films deposited by e-beam evaporation on Si substrate, 3 nm layer of chromium was interposed as adhesion layer. The experimental equipment was configured to have almost fully -45° linearly polarized light impinging the sample [28,29].

The optical scheme is shown in Fig.6: the beam reflected by the phase retarder element was analyzed by the polarizer and recorded by the CEM detector. Accordingly, the output signal is described as follows in terms of the Stokes parameters and Mueller matrix:

$$S^{\sim} = R(-\theta).M(FRP).R(\theta).M(WR).S_0 \quad (7)$$

where $M(WR)$ is the Mueller matrix of the phase retarder element and (R) are rotation matrices.
From a general point of view, the Mueller matrix of a reflector can be derived by describing its behavior as a polarizer with the amplitude reflection coefficients r_s^R and r_p^R, in series to a phase retarder with δ as delay:

$$M_{Retardar} = \begin{pmatrix} \frac{|r_S^R|^2 + |r_P^R|^2}{2} & \frac{|r_S^R|^2 - |r_P^R|^2}{2} & 0 & 0 \\ \frac{|r_S^R|^2 - |r_P^R|^2}{2} & \frac{|r_S^R|^2 + |r_P^R|^2}{2} & 0 & 0 \\ 0 & 0 & |r_S^R||r_S^R|\cos\delta & |r_S^R||r_S^R|\sin\delta \\ 0 & 0 & -|r_S^R||r_S^R|\sin\delta & |r_S^R||r_S^R|\cos\delta \end{pmatrix} \quad (8)$$

The properties of phase retarders and quarter wave plates can be described by the ellipsometric parameters, ψ and δ derived by ellipsometric measurements and defined by the following relationships [28,31]:

$$tan\psi = \frac{r_p}{r_s} \qquad \Delta = \delta_p - \delta_s \quad (9)$$

Back to the experiment, the light emitted by the deuterium lamp and going through the reflectometer was reflected by the sample under investigation, then the output intensity was analyzed by rotating the four-reflection polarizer. The detected intensity is described by the following relation:

$$\tilde{S_0} = \frac{1}{4}\begin{pmatrix} \left(\left(|r_s|^8 + |r_p|^8\right).\left(|r_s|_R^2 + |r_p^2|_R\right) + \left(|r_s|^8 - |r_p|^8\right).\left(|r_S^R|^2 - |r_p^R|^2\right)\cos 2\theta\right)S_0 \\ + \left(\left(|r_S^R|^2 + |r_p^R|^2\right).\left(|r_S^R|^2 - |r_p^R|^2\right) + \left(|r_s|^8 - |r_p|^8\right).\left(|r_S^R|^2 + |r_p^R|^2\right).\cos 2\theta\right)S_1 \\ +2\left(\left(|r_s|^8 - |r_p|^8\right)r_s^R r_p^R .\cos\delta.\sin 2\theta\right).S_2 \\ +2\left(\left(|r_s|^8 - |r_p|^8\right)r_s^R r_p^R .\sin\delta.\sin 2\theta\right).S_3 \end{pmatrix} \quad (10)$$

Eq. (10) can be conveniently rewritten in terms of the ratio $\frac{r_p}{r_s}$, in order to handle only three unknown parameters: the ratio, the phase δ, and the Stokes parameters S_i.

Aluminum sample was measured at four different incidence angles. The output intensity at each angle was recorded versus the rotation angle of the polarizer acting as analyzer (Fig.6).

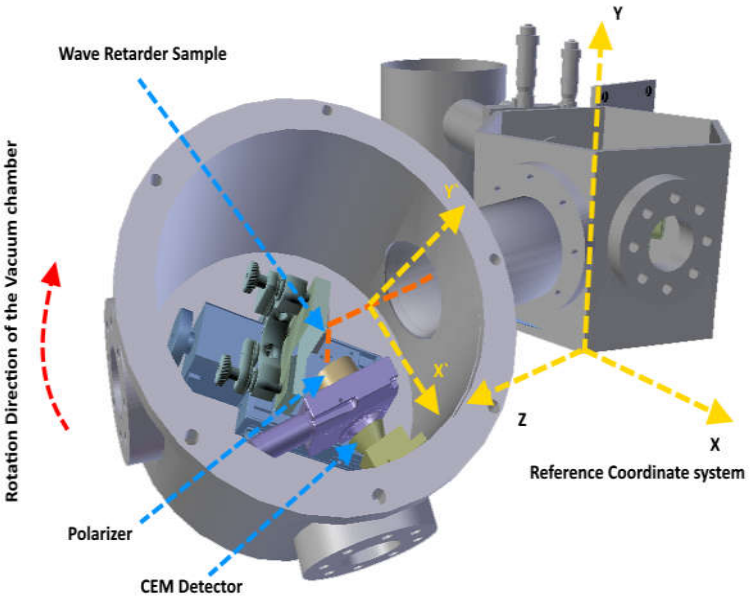

Fig.6. The experimental arrangement for testing a phase retarder by using the improved VUV-EUV normal incidence reflectometer facility.

In order to determine the parameters ψ and δ of the sample for each incidence angle and to estimate S_3, we performed the fitting procedure by using a MATLAB code based on the Levenberg–Marquardt algorithm and developed accordingly to Eq. (10). We defined the interval of existence for each free parameter and we performed the fitting procedure 300 times by randomly changing the starting guess of the parameters between the selected intervals. The standard deviations (STDV) were calculated over 300 iterations. The fitted and the measured curves are shown in Fig.7 and Fig. 8, the output values of the ellipsometric parameters are reported in Table 2.

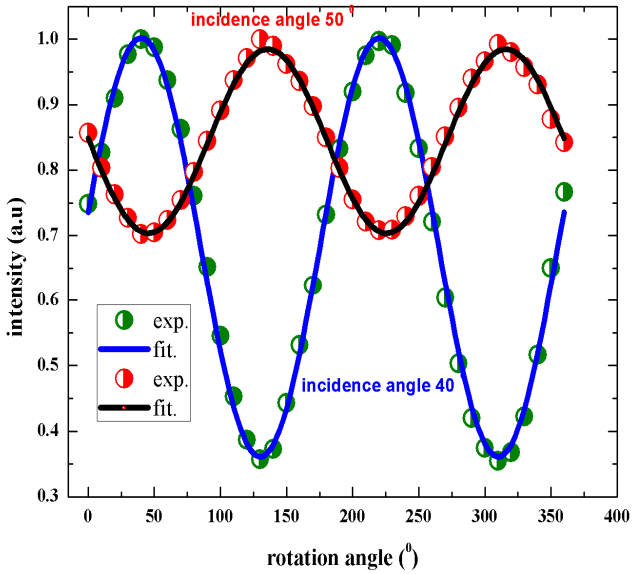

Fig. 7 Measured and fitted data of aluminum samples at two different incidence angels 40^0 and 50^0.

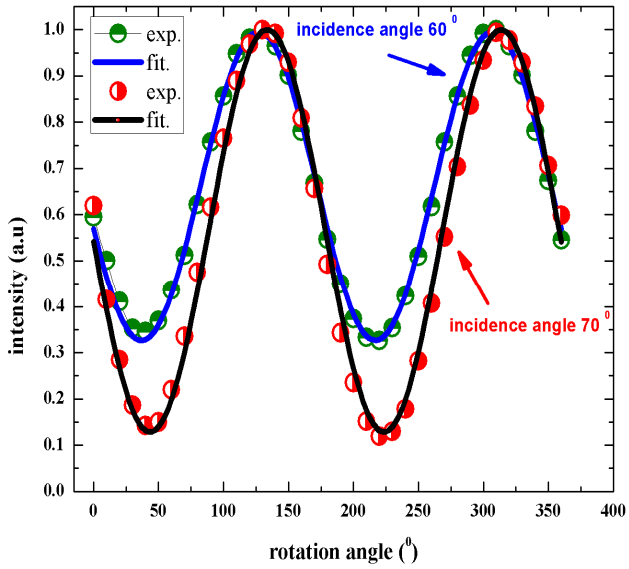

Fig. 8 Measured and fitted curves of aluminum samples at two different incidence angels 60° and 70°

Table 2. The fitted values of ratio, phase and S_3 with the standard deviation STDV.

Incidence angle	$\tan\psi = \frac{r_p}{r_s}$	STDV ratio	$\Delta\delta^0$	STDV $\Delta\delta^0$	S_3	STDV S_3
40	1.12	8.015e-007	68	6	0.02	0.12
50	1.08	1.963e-004	101	6	0.0005	0.0970
60	0.94	1.455e-005	120	6	-0.033	0.098
70	1.04	2.023e-007	142	5	-0.083	0.082

The approach allows a quite good estimation of S_3. The fourth Stokes parameter resulted to be rather small. It is reasonable by considering that the beam coming from the reflectometer is emitted by an incoherent source and results to be almost fully linearly polarized.

The ellipsometric parameters of the sample can be determined quite accurately. The uncertainty associated to the phase is 3% - 9% depending on the incidence angles, while the uncertainty for the ratio is negligible. We use the phase derived by the ellipsometric measurements in order to retrieve the properties of the sample under investigation and to evaluate the potential of the method and the experimental system capabilities.

Aluminum is well known to have a thin oxide layer on its surface due to the reaction with air which strongly affects the optical properties of the film [23]. We fitted the phase experimental data by using IMD software [32] in order to retrieve the thickness of the oxide layer. We used the reported optical constants of Palik [32] for both Al and Al_2O_3. Fig. 9a shows the measured phase versus the incidence angle at wavelength 121.6 nm and the fitted curve by IMD, the determined structure (inset Fig.9a). The thickness of the oxide layer determined by the fitting procedure is 3.18 nm (χ^2=0.29).

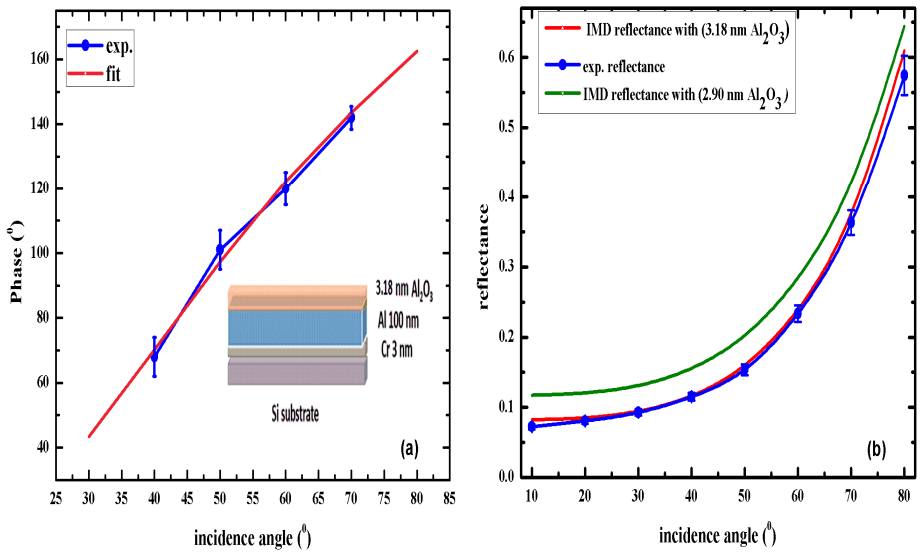

Fig. 9. a) Phase shift of aluminum sample versus incidence angle at 121.6 nm wavelength; the measured data were fitted by IMD software in order to determine the thickness of the oxide layer on top of aluminum surface. b) Reflectance measurements and simulation by IMD of aluminum sample assuming Palik's optical constants, the structure in inset of panel, and sharp interfaces.

Additionally, we performed the specular reflectance measurements of the sample at the same wavelength to verify the result obtained by analyzing the phase. Fig. 9b shows the experimental and the simulated reflectance of the determined structure. The data are in good agreement.

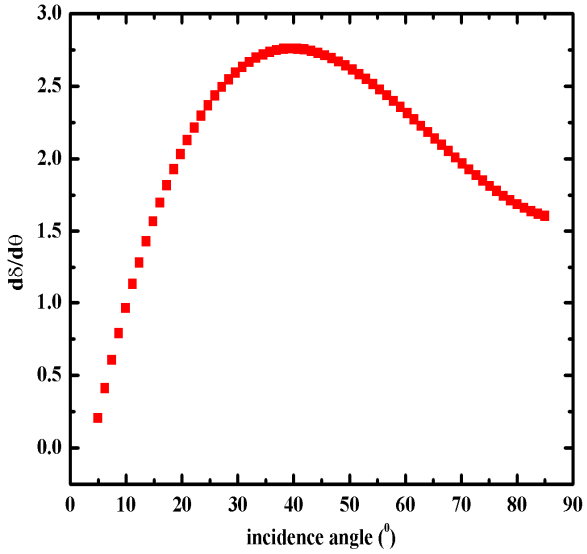

Fig. 10. Theoretical phase difference derivative vs incidence angle for the structure shown in the inset of Fig. 9a.

In order to verify the reliability and accuracy of the method, Table 3 shows the fitted parameters derived by the ellipsometric measurements compared with the results of the phase fit performed by IMD with Palik's optical constants.

The deviations between the values obtained from the ellipsometric measurements and the IMD ones can be reasonably attributed to small variations in optical constants, due to the samples fabrication process and storage, and experimental alignment errors. In terms of the structure of the sample, the sensitivity in determining the thickness of the aluminum oxide is estimated to be 0.3 nm. Such sensitivity comes out by analyzing the trend of the ratio that requires thinner oxide thickness (2.90 nm instead of 3.18 nm) to be matched. The simulated ratio and phase corresponding to 2.90 nm of Al_2O_3 on top of the Al film and retrieved by IMD and Palik's optical constants are reported in Table 3. The corresponding reflectance is graphed in Fig. 9b (green curve). We highlight that the sensitivity could be improved by adding further analysis.

Table 3. The fitted parameters obtained by MATLAB Code compared with those retrieved by IMD software.

Incidence angle	Phase fitted by IMD software Al_2O_3 thickness 3.18 nm		Simulation by IMD software Al_2O_3 thickness 2.90 nm		Fitted data by using ellissometirc measurements (MATLAB code)	
	$\tan\psi = \frac{r_p}{r_s}$	$\Delta\delta°$	$\tan\psi = \frac{r_p}{r_s}$	$\Delta\delta°$	$\tan\psi = \frac{r_p}{r_s}$	$\Delta\delta°$
40	1.20	71	1.10	65	1.12	69±6
50	1.24	98	1.13	92	1.08	101±6
60	1.21	122	1.13	117	0.94	120±6
70	1.14	143	1.09	139	1.04	142±6

It is worth mentioning that the proposed method takes into account the uncertainty of the whole system, including the uncertainty associated to the polarization state of the radiation delivered by the EUV ellipsometer. It was possible thank to the approach based on the Stokes formalism and the Mueller matrices.

Proof is the experimental results described in this paper about the properties of the aluminum optical coating: the oxide layer thickness was determined by fitting the phase retrieved by the ellipsometric measurements. As for aluminum in the determination of the oxide layer, the proposed method is suitable to be used for the study of physical and structural properties of any VUV/EUV reflective coating. Obviously, complex studies require proper ellipsometric models in order to rightly interpret the experimental data and derive the desired parameters. Concerning the aluminum film, the sample has an oxide layer due to exposure to air as expected. The oxide layer reduces the reflectance of the sample and changes the phase shift properties: for example, the bare Al coating acts as QWRs a 59° incidence angle, while the Al_2O_3 sample works at ~47°. However, the scientific literature demonstrated good stability of this type of samples once the oxide is formed and the sample under investigation actually exhibits good properties as phase retarder. The performances strongly depend on the incidence angle as it is shown in Figure 10, where the first derivative of the simulated phase difference respect to the incidence angle is reported. It is worth to note that small angular displacements can induce considerable phase deviation. Then an accurate alignment of the sample is required. This is especially true around 47.5° where, as we already said, the sample acts as a QWR with a phase shift of 90° and a ratio close to 1 and where small incidence angle deviation can induce phase variations of about 2.7°.

Considering the results, we can assert that:

- an ellipsometric method based on the Stokes formalism and Mueller matrices has been tested and experimentally verified;
- polarimetric properties of an Al sample with a layer of native oxide on the top were experimentally tested and characterized by using the proposed arrangement and method analysis;
- the Al_2O_3/Al specimen behaves as QWR at 47.5° incidence angle and 121.6 nm wavelength. It can be useful element for implementing optical system devoted to metrology and to change the polarization state of VUV/EUV radiation.

4. Conclusion

In summary, we have implemented and characterized an EUV reflectometer facility for polarimetric measurements in 90-160 nm spectral range. The reflectometer was coupled with a four reflection EUV linear polarizer in order to be used as a table top EUV ellipsometer system. The equipment was tested to characterize the optical and structural properties of Al_2O_3/Al sample as phase retarder by deriving its amplitude component and phase difference. The system can be a very promising laboratory equipment, simple alternative tool for fast and preliminary experiments compared to measurements sessions at large scale facilities. It is suitable to characterize phase retarders, polarizers and other optics in the EUV region and to investigate the properties of thin films, optical coatings and multilayer structures as it has been proved for the sample under investigation. Furthermore, the Al_2O_3/Al specimen behaves as QWR at 47.5° incidence angle and 121.6 nm wavelength and can be used for implementing optical system devoted to metrology and to manipulate the polarization state of VUV/EUV radiation.

PART 3 - PUBLICATIONS

List of publications on international journals

A.E.H. Gaballah, P. Nicolosi, Nadeem Ahmed, K. Jimenez, G. Pettinari, A. Gerardino, P.Zuppella "EUV polarimetry for thin film and surface characterization and EUV phase retarder reflector development" optics express(2017) (submitted)

A.E.H. Gaballah, P. Nicolosi, P.Zuppella, Nadeem Ahmed, K. Jimenez, G. Pettinari, A. Gerardino , P. Nicolosi "ellipsometric charcterization of QWR based on SnTe/Al structure in FUV range" proposed to be submitted to Optical Materials Express

Other publications by author

- Ashery, G. Said, W. A. Arafa, **A. E. H. Gaballah**, and A. A. M. Farag, "Structural and optical characteristics of PEDOT/n-Si heterojunction diode," Synthetic Metals, vol. 214, pp. 92-99, 2016.
- Ashery, G. Said, W. A. Arafa, **A. E. H. Gaballah**, and A. A. M. Farag, "Morphological and crystalline structural characteristics of PEDOTTM/TiO2 nanocomposites for applications towards technology in electronic devices," Journal of Alloys and Compounds, vol. 671, pp. 291-298, 2016.
- Ashery, A. A. M. Farag, **A. E. H. Gaballah**, G. Said, and W. A. Arafa, "Nanostructural, optical and heterojunction characteristics of PEDOT^{TM}/ZnO nanocomposite thin films," *Journal of Alloys and Compounds*, vol. 723, pp. 276–287, 2017

List of publications on conference proceedings

A.E.H Gaballah, P. Zuppella, A.J. Corso, P. Nicolosi "Optical and structural characterization of reflective quarter wave plates for EUV range" Proc. SPIE 9905, Space Telescopes and Instrumentation: Ultraviolet to Gamma Ray (2016).

A.E.H. Gaballah, Zuppella, Nadeem Ahmed, K. Jimenez, G. Pettinari, A. Gerardino , P. Nicolosi, "A table top polarimetric facility for the EUV spectral range: implementations and characterization" Proc. 10235, UV and X-ray Optics: Synergy between Laboratory and Space (2017).

K. Jimenez, **A.E.H. Gaballah**, Nadeem. Ahmed, P. Zuppella, P. Nicolosi "Optical and structural characterization of Nb, Zr, Nb/Zr, Zr/Nb thin films on Si3N4 membranes windows. " Proc. 10236, Damage to VUV, EUV, and X-ray Optics (2017).

References and links

1. E. Allaria, B. Diviacco, C. Callegari, P. Finetti, B. M. Mahieu, J. Viefhaus, M. Zangrando, G. De Ninno, G. Lambert, E. Ferrari, J. Buck, M. Ilchen, B. Vodungbo, N. Mahne, C. Svetina, C. Spezzani, S. Di Mitri, G. Penco, M. Trovo, W. M. Fawley, P. R. Rebernik, D. Gauthier, C. Grazioli, M. Coreno, B. Ressel, A. Kivimäki, T. Mazza, L. Glaser, F. Scholz, J. Seltmann, P. Gessler, J. Grünert, A. De Fanis, M. Meyer, A. K. Knie, S. P. Moeller, L. Raimondi, F. Capotondi, E. Pedersoli, O. Plekan, M. B. Danailov, A. Demidovich, I. Nikolov, A. Abrami, J. Gautier, J. Lüning, P. Zeitoun, and L. Giannessi, "Control of the polarization of a vacuum-ultraviolet, high-gain, free-electron laser," Physical Review X **4**, 1–15 (2014).
2. G. Capobianco, M. Malvezzi, S. Fineschi, J. I. Larruquert, A. Giglia, J. A. Aznarez, G. Massone, G. Crescenzio, S. Nannarone, F. Frassetto, J. A. Mendez, L. Rodríguez-de Marcos, and P. Miotti, "Characterization of linear polarizers in the wavelength range 100-150 nm (VUV) for solar physics applications," Proc. SPIE **8862**, 88620Y (2013).
3. D. Wilson, D. Rudolf, C. Weier, R. Adam, G. Winkler, R. Frömter, S. Danylyuk, K. Bergmann, D. Detlev Grützmacher, C. M. Schneider, and L. Juschkin, "Generation of circularly polarized radiation from a compact plasma-based extreme ultraviolet light source for tabletop X-ray magnetic circular dichroism studies," Review of Scientific Instruments **85**,

(2014).
4. Z.-Y. Guo, S.-B. Xi, J.-T. Zhu, Y.-D. Zhao, L. Zheng, C.-H. Hong, K. Tang, D.-L. Yang, and M.-Q. Cui, "Measurement of the polarization for soft X-ray magnetic circular dichroism at the BSRF beamline 4B7B," Chin. Phys. C **37**, 18001 (2013).
5. M. F. Tesch, M. C. Gilbert, H.-C. Mertins, D. E. Bürgler, U. Berges, and C. M. Schneider, "X-ray magneto-optical polarization spectroscopy: an analysis from the visible region to the x-ray regime.," Applied optics **52**, 4294–310 (2013).
6. N. V. Edwards, "Status and Prospects For VUV Ellipsometry (Applied to High K and Low K Materials)," AIP Conference Proceedings **683**, 723–737 (2003).
7. J. Jung, J. Bork, T. Holmgaard, and N. a. Kortbek, "Ellipsometry," Aalborg University Projects 132 (2004).
8. T. Saito, K. Ozaki, K. Fukui, H. Iwai, K. Yamamoto, H. Miyake, and K. Hiramatsu, "Vacuum ultraviolet ellipsometer using inclined detector as analyzer to measure stokes parameters and optical constants - With results for AlN optical constants," Thin Solid Films **571**, 517–521 (2014).
9. T. Kihara, "Measurement method of Stokes parameters using a quarter-wave plate with phase difference errors.," Applied optics **50**, 2582–7 (2011).
10. D. Goldstein, *Polarized Light*, 2nd ed. (Marcel Dekker, 2003).
11. D. Cubric, D. R. Cooper, M. C. a Lopes, P. Bolognesi, and G. C. King, "Polarization measurements in the VUV region of synchrotron radiation," Meas. Sci. Technol. **10**, 554–558 (1999).
12. B. Vodungbo, A. Barszczak Sardinha, J. Gautier, G. Lambert, C. Valentin, M. Lozano, G. Iaquaniello, F. Delmotte, S. Sebban, J. Lüning, and P. Zeitoun, "Polarization control of high order harmonics in the EUV photon energy range.," Opt. Express **19**, 4346–4356 (2011).
13. T. Zama and I. Saito, "Calibration of absolute spectral radiance in UV and VUV regions by using synchrotron radiation," Journal of Electron Spectroscopy and Related Phenomena **144–147**, 1087–1091 (2005).
14. L. Nahon and C. Alcaraz, "SU5: a calibrated variable-polarization synchrotron radiation beam line in the vacuum-ultraviolet range.," Applied optics **43**, 1024–1037 (2004).
15. A. J. Corso, E. Tessarolo, P. Zuppella, S. Zuccon, M. Nardello, and M. G. Pelizzo, "Phase delay characterization of multilayer coatings for FEL applications," Proceedings of SPIE - The International Society for Optical Engineering **9207**, 1–6 (2014).
16. V. G. Horton, E. T. Ardkawa, R. N. Hamm, and M. W. Williams, "A Triple Reflection Polarizer for Use in the Vacuum Ultraviolet," Applied Optics **8**, 667 (1969).
17. C. Lin, S. Chen, Z. Chen, and Y. Ding, "Design of reflective quarter-wave plates in extreme ultraviolet," Optics Communications **347**, 98–101 (2015).
18. S. C. Gao, C. Lin, and Hua, "Design of broadband transmission quarter-wave plates for polarization control of isolated attosecond pulses," J. Opt. **17**, 75601 (2015).
19. P. Zhang, Y. Tan, W. Liu, and W. Chen, "Methods for optical phase retardation measurement: A review," Science China Technological Sciences **56**, 1155–1163 (2013).
20. J. Kim, M. Zukic, D. G. Torr, and M. M. Wilson, "Multilayer thin film design as far ultraviolet quarterwave retarders," Proc. SPIE **1742**, (1992).
21. M. A. MacDonald, F. Schaefers, R. Pohl, I. B. Poole, A. Gaupp, and F. M. Quinn, "A W: B4C multilayer phase retarder for broadband polarization analysis of soft x-ray radiation.," The Review of scientific instruments **79**, 25108 (2008).
22. A. E. H. Gaballah, P. Zuppella, A. J. Corso, and P. Nicolosi, "Optical and structural characterization of reflective quarter wave plates for EUV range," Proc. SPIE **9905**, 99053H (2016).
23. T. Saito, A. Ejiri, and H. Onuki, "Polarization properties of an evaporated aluminum mirror in the VUV region," Applied Optics **29**, 4538–4540 (1990).
24. D. Garoli, F. Frassetto, G. Monaco, P. Nicolosi, M.-G. Pelizzo, F. Rigato, V. Rigato, a

Giglia, and S. Nannarone, "Reflectance measurements and optical constants in the extreme ultraviolet-vacuum ultraviolet regions for SiC with a different C/Si ratio.," Applied optics **45**, 5642–5650 (2006).
25. "Deuterium lamps | Hamamatsu Photonics," http://www.hamamatsu.com/jp/en/3013.html.
26. "Dr. Sjuts Optotechnik GmbH - Channel electron multipliers and complete measurement systems," http://www.sjuts.com/Introduction_Principles.html.
27. "Rotation Stages," https://www.physikinstrumente.com/en/products/rotation-stages/.
28. W. B. Westerveld, K. Becker, P. W. Zetner, J. J. Corr, and J. W. McConkey, "Production and measurement of circular polarization in the VUV," Applied Optics **24**, 2256 (1985).
29. A. E. H. Gaballah, P. Zuppella, N. Ahmed, K. Jimenez, G. Pettinari, A. Gerardino, and P. Nicolosi, "A table top polarimetric facility for the EUV spectral range: implementations and characterization," Proc. SPIE **10235**, 102350X (2017).
30. H. G. Berry, G. Gabrielse, and a E. Livingston, "Measurement of the Stokes parameters of light.," Appl. Opt. **16**, 3200–3205 (1977).
31. S. Uschakow, A. Gaupp, M. Gerhard, M. MacDonald, and F. Schäfers, "Polarization properties of Mo/Si multilayers in the EUV range," Nuclear Instruments and Methods in Physics Research, Section A: Accelerators, Spectrometers, Detectors and Associated Equipment **710**, 120–124 (2013).
32. E. D. Palik, "Palik, Handbook of Optical Constants, Vol.2 (AP, 1991)(ISBN 0125444222).pdf," Proc Natl Acad Sci USA **2**, Vol 2 (1991).

[28/09/2017]

Student signature

Supervisor signature